

Nuclear Archaeology for Gaseous Diffusion Enrichment Plants

Sébastien Philippe and Alexander Glaser

Nuclear Futures Laboratory, Department of Mechanical and Aerospace Engineering, Princeton University, Princeton, NJ, USA

Gaseous diffusion was historically the most widely used technology for military production of highly enriched uranium. Since June 2013, all gaseous diffusion enrichment plants worldwide are permanently shut down. The experience with decommissioning some of these plants has shown that they contain large amounts of uranium particles deposited in the cascade equipment. This article evaluates the potential of using uranium particle deposition to understand and reconstruct the operating histories of gaseous diffusion enrichment plants. First, a squared-off cascade enrichment model is derived to estimate the enrichment capacity of a reference plant. Then, using a cross-flow filtration model, the mass of solid uranium particles deposited over time in the tubular separation membranes of the stage diffusers is calculated. Finally, potential techniques to characterize these uranium deposits and help reconstruct the operating history of the plant are assessed.

INTRODUCTION

Gaseous diffusion is an isotope separation method based on the molecular diffusion of a gaseous isotopic mixture through porous barriers (or membranes). In the case of uranium isotope separation, the processed gas is a mixture of uranium-238 and uranium-235 in uranium hexafluoride, UF_6 .

Gaseous diffusion was historically the most widely used uranium isotope separation method for the military production of highly enriched uranium (HEU) in Nuclear Weapons States (NWS). In the framework of nuclear archaeology,¹ and the development of new tools to verify the past production of nuclear fissile materials for military purposes in NWS, this article presents a

Received 22 July 2013; accepted 5 November 2013.

Address correspondence to Sébastien Philippe, Department of Mechanical and Aerospace Engineering, Princeton University, E-Quad, Olden St, Princeton, NJ 08544, USA. E-mail: sp6@princeton.edu

Table 1: List of gaseous diffusion enrichment plants that produced HEU for military purposes. Numbers are estimates, typically with an error of 20–40% (except for the declared U. S. Production).

Country	Name of Plant	Operating years	HEU production (metric tons)	% of national HEU production
U.S.	Oak Ridge	1945–64	491	47.0
	Portsmouth	1956–92	552	52.8
Russia	Novouralsk	1949–87	80	5.6
	Serversk	1953–93	65	4.4
	Zelenogorsk	1962–90	90	6.3
	Angarsk	1957–93	180	12.5
U.K.	Capenhurst	1954–62	11	100
France	Pierrelatte	1967–96	35	100
China	Lanzhou	1964–80	6	30
	Heping	1975–87	14	70

novel approach to reconstruct the operating history of Gaseous Diffusion enrichment Plants (GDPs).

As of June 2013, all GDPs worldwide have been shut down.² In many cases, decommissioning and dismantling those facilities is already underway, making the development of verification methods a timely and urgent matter before possibly important information is lost or involuntarily destroyed during the dismantlement activities. Table 1 lists the GDPs that were used to produce HEU for military purposes in the NWS.³ Overall 57% of the worldwide production of HEU was done using gaseous diffusion enrichment.

During the early decommissioning stages in the United States, the United Kingdom, and France, it was found that the plants were contaminated by large amounts of uranium solid deposits in the cascade equipment.⁴ The mass of these deposits can represent several metric tons of uranium at various enrichment levels held up in the components of the plant.⁵ The analysis of this large contamination could represent a tremendous source of information on the operating histories of GDPs, and largely motivated the study presented in this article.

Consequently, a two-steps approach was developed to reconstruct the production histories of GDPs. First, a simple mathematical model of a GDP cascade using a set of basic process parameters was derived to assess the HEU production rate of a particular plant. Second, the potential of nuclear forensic analysis of the uranium deposits found on contaminated equipment to reconstruct the plant history is examined. Knowing the HEU production rate and operating periods could give an approximation of the total amount of HEU produced in a particular plant, which could eventually be compared with production records.

To illustrate the methods and results, the French gaseous diffusion plant in Pierrelatte is used as an example throughout the article.

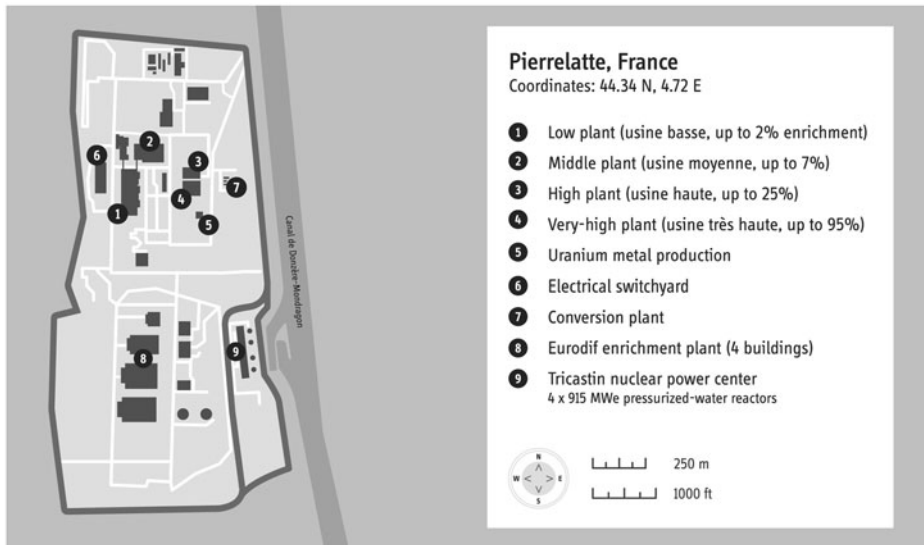


Figure 1: The Pierrelatte site layout: The military enrichment plant is situated in the northern part of the site, while the civilian enrichment plants, Eurodif George Besse I and II are located in the southern part. The proximity of both plants allowed the military plant to be supplied with LEU from the civilian plant starting in 1982.

MODEL OF THE PIERRELATTE GASEOUS DIFFUSION PLANT CASCADE

The Pierrelatte gaseous diffusion plant was designed to produce HEU for the French nuclear weapons and submarine reactors programs. The plant produced its first batch of HEU in April 1967 and was shut down nearly 30 years later on June 30, 1996.⁶ The original military requirements for Pierrelatte were to produce a minimum of 600–700 kg of weapon-grade HEU per year.⁷

The plant was composed of four main units called *usines* (“plants”) with each unit representing one step of a squared-off enrichment cascade. Figure 1 describes the plant layout.⁸ The first design projects from 1956 referred to a total of 2,500 stages for the four units.⁹ The low plant (*usine basse* or UB) was fed with natural uranium and enriched UF_6 up to 2% uranium-235, the middle plant (*usine moyenne* or UM) up to 7%, the high plant (*usine haute* or UH) up to 25%, and the very-high plant (*usine très haute* or UTH) to 90% and higher.¹⁰ The waste stream coming out of UB has been reported to have a tails assay of 0.35%,¹¹ though a higher tails assay of 0.5% uranium-235 has been reported for the early years of operation.¹² This higher level would be consistent with a strategy to produce HEU as fast as possible in the early years of the plant operation when production rate was limited by the available separative power.

In 1982, UB and 75% of UM were shut down after the civilian Eurodif gaseous diffusion plant, *George Besse* (GB), reached its full industrial production capacity.¹³ Afterwards, low-enriched uranium produced in the GB plant

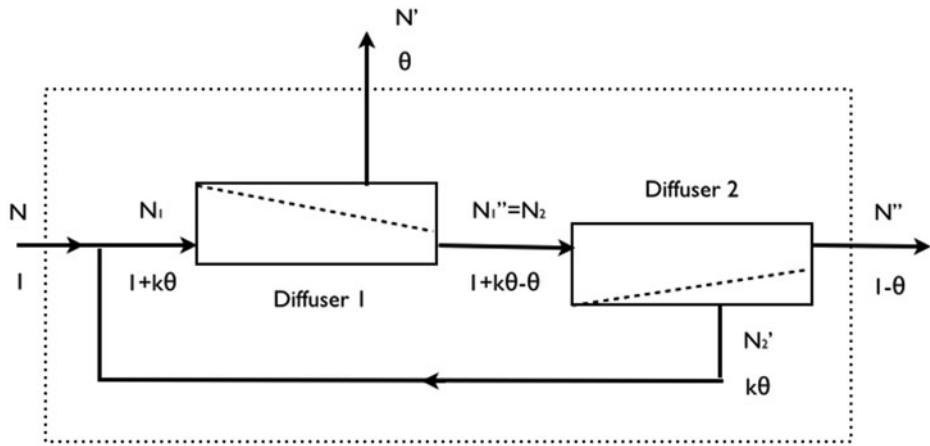


Figure 2: Enrichment stage with two diffusers. In this configuration, using $k = 1$ and $\theta = 0.5$, the overall stage separation factor and the separative power increase by 37.5% and 89%, respectively.

would be delivered to the Pierrelatte plant for further enrichment. Starting in 1984, the 1,328 stages of the three remaining plants (25% of UM, UH, and UTH) were operated every year on a seasonal cycle from April to October until the plant was completely shut down in 1996.¹⁴

Every single stage in the Pierrelatte plant was made of a compressor, a heat exchanger, and two diffusers.¹⁵ Each diffuser is made of thousands of small porous tubes. The two diffusers are connected together as shown on Figure 2. This configuration, which is equivalent to a single stage with internal recirculation, can increase the stage separation factor by 37.5% and the separative power by 89%.¹⁶ The average separation factor of a Pierrelatte plant diffuser was reported to be 1.0014.¹⁷ With the two diffusers design, the average stage separation factor would have been increased to 1.00193.

Each plant had its own type of diffusion barrier and stage compressor, all different from one another. All barriers in the plant were of the composite multilayer type: each tube was made of a thin porous layer deposited on top of a structural layer allowing the barrier to work in higher pressures.¹⁸ The high pressure in Pierrelatte's stages was about 0.2 atmospheres (atm).¹⁹ This pressure being under the critical pressure of UF_6 , the operating temperature of the flowing gas had to be kept at all time higher than 40 °C to avoid any solidification of UF_6 in the process equipment. As a consequence, the atmosphere inside the process building was kept at a temperature of 55 °C.²⁰

The following paragraphs focus on the low and the very high plants as both are of particular interest in this analysis. UB gives information on the feed and the tails of the plant. The design of UTH is directly related to the weapon grade HEU product output of the plant.

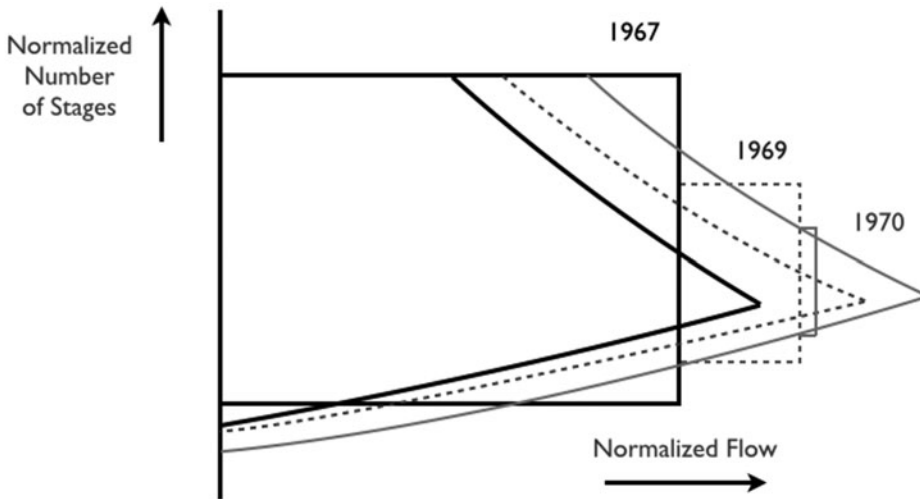


Figure 3: Historical squared-off and corresponding ideal cascade profiles of the low plant in the early years of the plant operation.

The Low Plant (UB)

The low plant started industrial production of LEU at a level of 2% in January 1965.²¹ The unit had a total of 480 stages in three 160-stages subcascades.²² The material flow was equal in all stages until 1969 when the original square cascade profile of UB was gradually modified to better match the profile of an ideal cascade around the feed introduction stage (see Figure 3).²³

The UB compressor is reported to be a single stage 150-kW supersonic compressor with a mass flow rate of 5 kg of UF_6 per second,²⁴ and a compression ratio of 8:1.²⁵ The equivalent uranium mass flow rate would be 1.07×10^8 kg of uranium per year.

The Very-High Plant (UTH)

UTH was the final step in the enrichment process, thus its characteristics determine and constrain the product output of the plant. The material flow in UTH was reported to be 60 times less than in UB, which will give a flow of 1.78×10^6 Kg of uranium per year.²⁶ 1,150 compressors were used in UTH, one for each stage.²⁷ Based on these two values for the stage flow rate and number of stages and further assuming a product enrichment level of 90% uranium-235, a feed enrichment level of 25% (from the previous step UH), and a stage separation factor of 1.00193, the stage equation of UTH (Equations [B.10] and [B.6] in Appendix B) is solved in order to find the product rate of the plant. The result gives a product rate of about 580 kg of weapon-grade HEU per year. In June 1995, some of the first compressors installed in UTH started to run over

200,000 operating hours without failure.²⁸ Assuming 200,000 hours of operation until June 1995, and adding 5,150 hours to account for further production until the Pierrelatte plant shut down in June 1996, a direct estimate of the total amount of weapon grade HEU produced at Pierrelatte would be 14 ± 2 tons of HEU. This amount is significantly lower than previously reported values in the literature, i.e., 35 ± 5 tons of weapon-grade HEU.²⁹ This lower estimate is based on the assumption that the high plant (UH) did not produce additional amounts of 25%-enriched material but there is no evidence that France has used such material for any military or other purposes.

Model of the Pierrelatte Cascade and Results

Various assumptions are made to construct a simple model of the Pierrelatte cascade. The arrangement is assumed to be a squared-off cascade with four different steps representing the four units of the plant. The stripping section of the plant is located in the low plant. The enrichment levels at the output of each step are 2%, 7%, 25%, and 90% uranium-235. The feed and tails assay are respectively 0.7% (natural uranium) and 0.5% uranium-235 as reported earlier.³⁰ An average separation factor α is set for all the stages and equal to 1.00193. The product rate of the plant is assumed to be 600 kg of 90% uranium-235 per year. The equations used to obtain the squared-off cascade model are detailed in Appendix B. The last assumption made is related to the optimization criterion of the stage equation of a squared-off cascade.

The stage equation relates the number of stages, S_i , with the normalized flow rate ψ_i , in each step, i , of the squared-off cascade:

$$S_i = f(\psi_i, \alpha, N_i, N_{i-1}, N_P) \quad (1)$$

with N_i and N_{i-1} being respectively the product and feed concentration of the i -th step and N_P , the plant product concentration.

This equation has an infinite number of solutions. To identify a unique solution requires using an optimization criterion. In this model, the criterion chosen minimizes the total flow rate per mole of product. Optimization is usually performed on the cost function of the cascade in order to minimize the production cost of the enriched uranium.³¹ Nevertheless, the assumption made here is ideal for minimizing the energy consumption of the cascade and increasing its efficiency and should give a good order-of-magnitude estimate for the material flow in each step.

The flow pattern in the Pierrelatte cascade is shown in Figure 4. The solid line represents the ideal cascade shape of the plant;³² the dashed line, the equivalent squared-off cascade obtained with the parameters presented earlier.³³

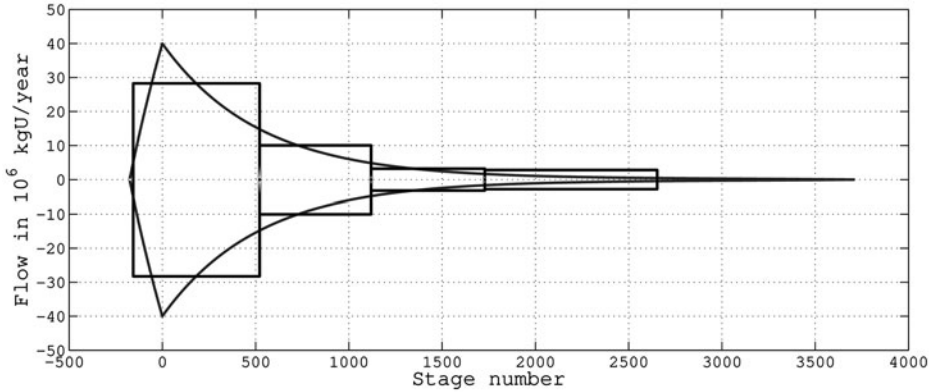


Figure 4: The Pierrelatte ideal cascade and equivalent squared off cascade obtained using the model described in Appendix B.

Table 2 summarizes the results. The separative power for each step i is calculated using the following equation:

$$U_i = \frac{1}{2}L_iS_i(\alpha - 1)^2 \tag{2}$$

The model represents only the production of HEU at 90% uranium-235 in Pierrelatte. It is important to note that the real capacity of the plant is likely to be higher, taking into account additional product streams at lower enrichment levels. These product streams, used, for example, to produce LEU for naval reactor fuel, are omitted from the calculations due to the absence of information concerning them in the literature. While important, additional LEU production is of secondary relevance for an estimate of France’s HEU stockpile.

Another difference between the model and reality may include the evolution over time of the lower part of the cascade. The tails assay was initially

Table 2: Results of the squared-off cascade model for Pierrelatte in the early operational years. Product, feed and tail assays are respectively 90%, 0.7% and 0.5% uranium-235.

Plants	Number of stages	Material flow rate (10 ⁶ kg of uranium per year)	Separative power-SWU (10 ³ kg per year)
Low	679	56.5	71.5
Middle	597	20.1	22.3
High	610	6.4	7.3
Very high	924	5.6	9.6
Total	2810	—	110.7

0.5% uranium 235, but is likely to have been lowered at some point. The fact that, after 1984, the Eurodif plant effectively replaced the lower part of the plant also may have an impact on this estimate. Finally the largest discrepancy may come from the optimization criterion chosen to solve the squared-off cascade equations. In the model, the total flow rate per mole of product is minimized which is equivalent to minimizing the total separation power in every step of the cascade per mole of product, which could lead to an underestimation of the separative power of the whole cascade. All things considered, previous estimates have put the total plant capacity at about 300,000 SWU per year.³⁴ One 1996 publication authored by CEA officials quotes the capacity as “a few 100,000 SWU per year.”³⁵

The following section looks at the origin of solid uranium contamination in GDP equipment, models the particle deposition mechanism in diffusers and assesses the potential of using nuclear forensics techniques on deposited particle as a new tool to reconstruct the operating history of GDPs.

THE ORIGINS OF SOLID URANIUM CONTAMINATION IN GDP EQUIPMENT

Uranium hexafluoride is a highly reactive molecule. Reduction of UF_6 during contact with exposed steel surfaces will produce various solid uranium compounds such as UF_4 , UF_5 and U_2F_9 .³⁶ The hydrolysis of UF_6 by water is almost instantaneous and produces gaseous HF and solid particles of UO_2F_2 . These reactions are not only a source of losses of UF_6 , but are responsible for deposits and corrosion in the plant equipment as well as the clogging of the separation barriers.³⁷ It is of the utmost importance for a viable plant design that the in-leakage of moisturized air or any type of lubricant oils in the process equipment is kept as low as possible, but contamination of the equipment is inevitable under realistic conditions and over longer periods of time. Among all the equipment, the diffusion barrier is the most sensitive to uranium deposition. Acting as a cross-flow filter, the porous membrane traps most of the suspended uranium solid particles carried by the UF_6 flow (Figure 5).³⁸ In the Pierrelatte plant, 80% of the deposited uranium was located in the diffusers. After various chemical cleaning processes were used to remove most of the solid deposits, it was estimated that 3 metric tons of uranium at various enrichment level would not be recoverable and be disposed along with the associated process equipment in appropriate nuclear wastes storage facilities.³⁹

It is interesting to note that in the US Portsmouth plant, where reprocessed uranium was used as a feed material, the barriers are not only contaminated by uranium compounds, but also by traces of various other actinides (i.e., Th, Np, Pu, Am) and fission products (such as Tc-99).⁴⁰ All those elements

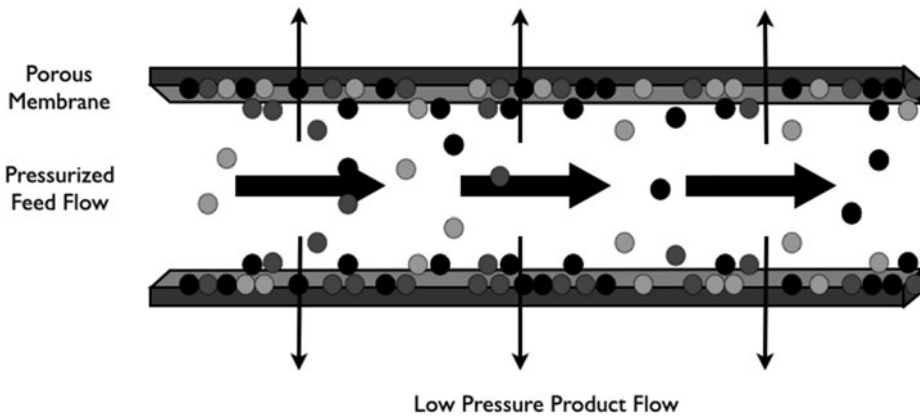


Figure 5: Cross flow filtration: solid particles accumulation on the porous surface due to the influence of the large pressure gradient across the membrane.

are carried with material flow under the form of binary-hexafluoride molecules (i.e., ThF_6 , NpF_6 , PuF_6 , AmF_6 and TcF_6).

MODEL OF UO_2F_2 DEPOSITION IN PIERRELATTE DIFFUSERS

The annual UO_2F_2 deposition rates in the stage diffusers of a gaseous diffusion enrichment plant are estimated below in order to determine if methods of nuclear forensics could be used to reconstruct the plant throughput based on a particle deposition model and the data presented in the previous sections. UO_2F_2 is not the only uranium solid compound to be found in barriers but its presence in the gas stream has the advantage to be directly related to the moisturized air in-leakage in the equipment, making it a good candidate for this analysis.

Model of UO_2F_2 Deposition on a Porous Tubular Membrane

The deposition mechanism of solid particles on the membrane is similar to the concept of cross-flow filtration. As UF_6 is processed in the diffuser, about half of the entering flow (corresponding to the stage cut) diffuses through the membranes. The pressure difference across the thickness of a porous tubular membrane induces a radial velocity that is responsible for the accumulation of solid particles in the boundary layer. Due to this phenomenon, micron-sized particles impact on the membrane and can remain trapped in the diffuser. The theory predicts that, ultimately, an equilibrium thickness of the layer is reached,⁴¹ but with the assumed flow conditions, low concentration of suspended particles, and assuming normal operations (i.e., no accidental leaks), the layer thickness will always stay far away from this equilibrium value. In

the event of an accidental leak, it is believed that the clogged barriers would be improper to use and replaced during maintenance operations. Therefore the rate at which the mass of deposited particles increases can be simply assumed to be linearly proportional to the particle concentration entering the diffuser,⁴² the stage cut, and the volumetric flow rate of UF_6 in the tubular membrane. The particle deposition rate can be written as follows:

$$\dot{m}_{UO_2F_2} = \theta \cdot C \cdot Q_{UF_6} \quad (3)$$

with θ the “stage-cut,” C the solid particles concentration and Q_{UF_6} the UF_6 volumetric flow rate.

UO_2F_2 Particles Concentration in the Flow

The presence of UO_2F_2 is due to the hydrolysis of UF_6 by water when ambient moisturized air leaks into the process equipment. When HF obtained from this reaction comes into contact with oxides, it regenerates water leading to further decomposition of UF_6 .⁴³ In the following, it is assumed that all water entering the process equipment reacts with UF_6 . In order to find the concentration of particles of UO_2F_2 in the UF_6 flow, several inputs are needed: the temperature, pressure and humidity of the air inside the process building as well as the in-leakage rate in the equipment.⁴⁴ For the Pierrelatte plant, two different values for the tolerated in-leakage allowed in the process (related to the flow of gas entering the equipment by porosity) were reported to be 2×10^{-2} and 10^{-4} liter-millitorr per second (lusec) and m^3 of volume occupied by UF_6 .⁴⁵ The equations used to convert the air in-leakage values to a UO_2F_2 particles concentration in the flow are presented in Appendix C.

Actual Deposition Rate during the First Two and a Half Years of Operation

Between 1967 and 1968, about 2.5 years after LEU production started in Pierrelatte, all UB separation barriers were replaced. The official explanation was to improve the efficiency of the plant.⁴⁶ The 5.04 million disposed barrier tubes were buried in the ground on the plant site.⁴⁷ The barriers were contaminated by solid UF_5 , UF_4 and UO_2F_2 . The mass of deposited uranium per surface area was 10 to 20 g/m^2 with an enrichment level between 0.5% and 2% uranium-235. The mass was about equally distributed between the UF_5 , UF_4 and UO_2F_2 when the barriers were buried.⁴⁸ Every barrier had a unit area of 235 cm^2 and a weight of 126 g.⁴⁹ The tube length is reported to be approximately 50 cm with 8 tubes giving the diffuser length.⁵⁰ Assuming 480 stages and two diffusers per stage, one diffuser would contain 5250 barrier tubes. The average mass of UO_2F_2 deposited per single membrane tube can then be easily calculated and is found to be between 0.1 and 0.2 g;⁵¹ giving a deposition rate

of 40–80 mg of UO_2F_2 per year per tube of the Low Plant (UB).⁵² This is equivalent to a deposition rate of 1.7–3.4 g of UO_2F_2 per year per m^2 of membrane with a fraction of uranium deposited in UO_2F_2 form over the mass of uranium processed through the membrane of 9×10^{-12} .

Expected UO_2F_2 Deposition Rate from the Model

Using the tube geometry defined in the previous paragraph, and a rate of air in-leakage in the process equipment equal to 2×10^{-2} lusec, yields a particle concentration of 3.6×10^{-12} kgm^{-3} of UO_2F_2 in the flow, which leads to a deposition rate of 0.13 mg of UO_2F_2 per year and per tube. This corresponds to the deposition of 5×10^7 one-micrometer diameter spherical particles of UO_2F_2 every year.⁵³

NUCLEAR FORENSICS ANALYSIS OF THE DEPOSITED PARTICLES

The previous results indicate that the large amount of UO_2F_2 particles trapped over time is sufficient to perform nuclear forensic analysis on barrier samples. With this assumption, it should be possible to obtain relevant information even from a single tube, i.e., one out of several million tubes.

Bulk analysis of a selected tube would give information on enrichment levels, including uranium-235/uranium-238 and uranium-234/uranium-238 ratios, making it possible to locate quite accurately the position of the tube in the enrichment cascade. If a large number of samples are available, it could be used to fit a squared off cascade model, allowing to obtain a good approximation of the cascade shape and normalized production rate. These results could be correlated for example with the mechanical analysis of a stage compressor to estimate the maximum production rate of the cascade.

The large available amount of uranium also may allow an age-dating of the deposited particles using for example the thorium-230/uranium-234 chronometer.⁵⁴ Figure 6 shows the predicted amount of uranium-234 atoms on a single tubular membrane in UTH for three different scenarios. The first scenario represents the production scenario in Pierrelatte obtained from the literature (full production from 1967, then seasonal production from 1982 to 1996). The second scenario assumes full HEU production in Pierrelatte for the plant lifetime. The third one is another hypothetical scenario assuming constant production over lifetime and ending with the same uranium-234 inventory in 1996 as the second scenario. By combining these three uranium-234 inventories with their respective thorium-230/uranium-234 chronometer ratios [4.09×10^{-5} , 3.55×10^{-5} and 4.09×10^{-5}], it is possible to distinguish between these scenarios. A bulk analysis of the particles recovered from a single diffuser tube may therefore be sufficient to discriminate between different possible production

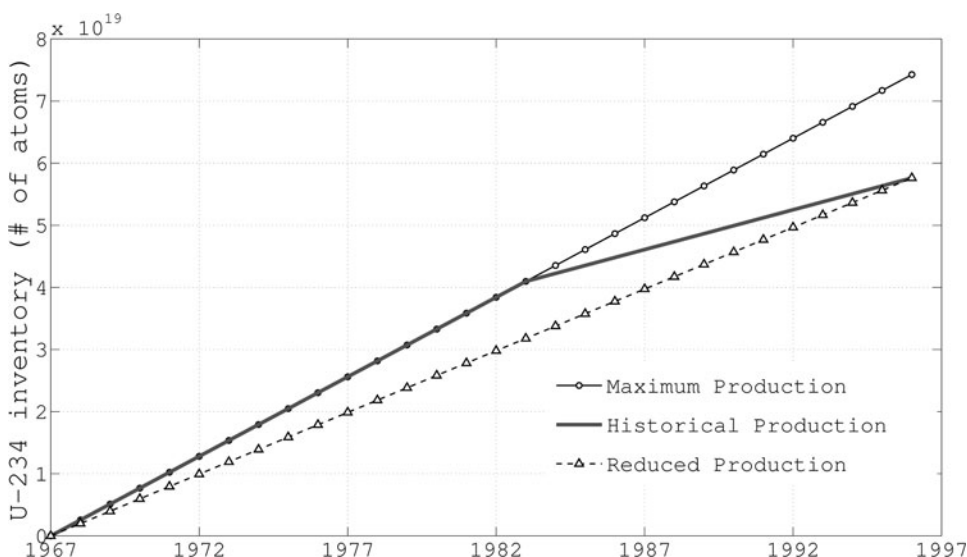


Figure 6: Uranium-234 inventory on a single tubular membrane for three different scenarios. The solid line represents the declared historical production in Pierrelatte. The round-dotted line represents the maximal production scenario during the plant lifetime. The dashed line with triangles represents constant production over lifetime ending with the same uranium-234 inventory as the historical production scenario.

histories and help confirm the correctness *and* completeness of a plant-specific fissile-material declaration.

Furthermore, if the forensic team has the ability to select individual particles or perform statistical sampling on a membrane, it would in principle be possible to reconstruct the complete production history of the stage and, by extension, the cascade. Each UO_2F_2 particle has a particular thorium-230/uranium-234 ratio, registering a particular time at which the cascade was operating. Therefore, the continuous contamination of the membrane during production will “store” the operating history in the deposited particle on the membrane surface. The time resolution needed to obtain a clear history would be of the order of 2–3 months, allowing the analysis to distinguish between production periods and longer-term shut downs. The ability to analyze particles individually would be extremely valuable for the nuclear archaeology of GDPs. The amount of particles available for analysis appears sufficient even with a partial loss of information due to the impact of the decommissioning process that is discussed below.

IMPACT OF THE DECOMMISSIONING PROCESS

During the dismantlement of the gaseous diffusion plants, various steps can affect the ability to characterize and study the uranium deposits. The main

difficulties for an effective archaeological analysis arise from the decontamination of the plant and removal of bulk uranium deposits, both of which may be required or preferable for environmental reasons. Moreover, an analysis could be limited by the ability to access discarded process equipment after it is sent away either for recycling or to nuclear waste storage facilities.

Cleaning Process

One of the first steps taken during the decommissioning process is the attempt to remove most of the uranium compounds deposited in the cascade stages. If the plant is not yet shut down, gaseous decontamination can be used to remove a large part of the deposits. Plant operators can inject a fluorinating agent (for example, chlorine trifluoride ClF_3 or nitrogen trifluoride NF_3) into the cascade. The ClF_3 dissolves primarily the bulk deposits of UO_2F_2 and removes it as UF_6 which is later recovered.⁵⁵ In Pierrelatte, this operation together with the initial removal of the UF_6 inventory was conducted right after the production ended in June 1996, and took one and a half years for UH and UTH to be complete.⁵⁶ The next step is then to dismantle all cascade equipment that was in contact with UF_6 using either chemical or mechanical removal techniques for additional decontamination. The cleaning process significantly reduces the amount of deposited material. A recent article published by researchers at the *Commissariat à l'Énergie Atomique* indicates that cleaning processes (aspiration, high pressure cleaning, and bath) used on the compressors of the low plant (UB) reduced the contamination from 18 g to 9 g of uranium-235 mostly in solid UF_4 form.⁵⁷ This corresponds to a remaining amount of about 900 grams of total UF_4 per compressor available for analysis, making them a good alternative candidate to gain information on the production history if separation membrane would remain classified objects. Additional data related to the impact of decontamination are known to be available; for example, from the U.S. cascade improvement and cascade upgrade programs.⁵⁸

Accessibility of the Dismantled Materials

One of the economic incentives of GDP dismantlement is the ability to recycle metals to sell them as clean scrap to the metal markets. This includes large quantities of aluminum or steel. Whether or not decontaminated metals can be directly sold after decontamination varies from one country to another based on national legislation. In the United Kingdom, the legislation permits to do so when the waste activity gets under a particular level (usually expressed in Becquerel per kg); thus from the 160,000 tons of metal and concrete making up the structure and contents of the Capenhurst diffusion plant, 99% were recycled as clean material. Only equipment for which decontamination was

not economically viable was sent to low-level radioactive waste storage;⁵⁹ this would be the only one available for an analysis of deposited particles. Whether or not the remaining equipment from Capenhurst includes diffusion barriers is unknown to the authors.

In France, the legislation is much different. Even for very low activity wastes, there is no activity limit under which wastes can be considered as usual industrial wastes; thus the reintroduction of those materials on the market is currently forbidden,⁶⁰ giving the potential to access these materials for the study of deposited particles. As discussed earlier in this paper, in the Pierrelatte plant, 80% of the uranium residual mass was held in the diffusers. During the dismantlement, after being removed from the stages of the different units of the plant, the porous barriers tubes were grinded, mixed together, then sealed in concrete to finally be shipped in nuclear waste storage facilities making them extremely difficult to be recovered at a later stage.⁶¹

CONCLUSION

This article examines a new approach for the reconstruction of the operating histories of gaseous diffusion enrichment plants. By using a simple model for the reconstruction of a squared-off cascade and evaluating the potential of a nuclear forensic analysis of the large amount of uranium deposited in the process equipment, especially in the diffusion barriers, it has been shown that it should in principle be possible to make good estimates of a gaseous diffusion enrichment plant production capacity, including separative power and operating periods. These results can then be compared, for example, to material production records made available by nuclear weapon states as part of a transparency initiative or an arms-control verification regime. This would help build confidence on how much enriched uranium was produced in a particular plant.

During the dismantlement of a gaseous diffusion plant, the various types of cleaning processes, which generally are required to reduce environmental concerns, have a strong impact on the nature and quantity of recoverable deposits. Countries with dismantlement experience could contribute to characterize this impact more precisely. The ability to access dismantled contaminated equipment could be essential to perform a meaningful nuclear archaeological analysis. Since all gaseous diffusion plants are now shut down, it would be important for countries to keep some intact contaminated diffusion barriers for future analysis or to carefully characterize these barriers before disposition. Overall, the findings presented in this article suggest that equipment from gaseous diffusion plants, especially the diffusion barriers, could be a unique source of information for future nuclear archaeology that could help verify the completeness of fissile material production histories.

States with shut down gaseous diffusion plants could help validate the concepts of nuclear archaeology presented in this article. Experimental work including the characterization of deposits, age-dating of individual particles deposited on separation membranes, and reconstruction of key plant design parameters such as moisturized air-in-leakage rates to validate the deposition model are of particular importance. These exercises could potentially be conducted through international collaboration, perhaps also including non-weapon states, promoting the importance of nuclear archaeology as a tool for verifying baseline declarations of historic fissile material production.

NOTES AND REFERENCES

1. Steve Fetter, "Nuclear Archaeology: Verifying Declarations of Fissile Material Production," *Science & Global Security* 3 (1993): 237–259.
2. Operation of the George Besse I plant (Eurodif) ended in 2012, and the Paducah plants ceased uranium enrichment operation in May 2013. Both plants were producing low enriched uranium.
3. The data in Table 1 are obtained from various sources. The United States made official declarations in 2006, U.S. Department of Energy, *Highly Enriched Uranium: Striking a Balance. A Historical Report on the United States Highly Enriched Uranium Production, Acquisition, and Utilization Activities from 1945 through September 30, 1996*, (2001): 1–174, <www.ipfmlibrary.org/doe01.pdf>. Estimates for Russia are based on: Pavel Podvig, "History of Highly Enriched Uranium Production in Russia," *Science & Global Security* 19(1) (2011): 46–67. Data for the individual plants were kindly shared by the author Pavel Podvig (personal communication, November 2013). The United Kingdom declared its HEU stockpile in 2006. This stockpile includes a significant amount supplied by the United States. The U.K. declaration does not specify the amount of HEU produced domestically at the Capenhurst plant. The estimate is from: International Panel on Fissile Materials, "Global Fissile Material Report 2010, Balancing the Books: Production and Stocks," (2010): 71–76, <www.fissilematerials.org/library/gfmr10.pdf>. Estimates for France are based on: International Panel on Fissile Materials, Balancing the Books: Production and Stocks. However, the results obtained in this paper offer a new technical basis for a significantly lower estimate. This is further discussed in International Panel on Fissile Materials, "Global Fissile Material Report 2013, Increasing Transparency of Nuclear Warhead and Fissile Material Stocks as a Step toward Disarmament," (2013): 12–13 <www.fissilematerials.org/library/gfmr13.pdf>. Estimates for China are based on: International Panel on Fissile Materials, Balancing the Books: Production and Stocks, *op. cit.*, 97–102.
4. For the United States see: Committee on Decontamination and Decommissioning of Uranium Enrichment Facilities, National Research Council, *Affordable Cleanup? Opportunities for Cost Reduction in the Decontamination and Decommissioning of the Nation's Uranium Enrichment Facilities* (Washington, DC: The National Academies Press, 1996): 35–41, <www.nap.edu/openbook.php?record_id=5114&page=R1>; For the United Kingdom, see: S. G. Baxter and P. Bradbury, "Decommissioning of the Gaseous Diffusion Plant at BNFL Capenhurst," in WMS Papers (presented at the Waste Management Symposia, Phoenix, AZ, 1991): 735–737; For France, see: Pascal Bourrelier and Charles Kassel, "Le Démantèlement Des Usines Militaires de Pierrelatte," *Annales Des Mines* (July 1999): 37–43.
5. Pascal Bourrelier and Charles Kassel, *op. cit.*, 41.

6. Pascal Bourrelier and Charles Kassel, *op. cit.*, 37–38.
7. Jean-Pierre Daviet, Eurodif: *Histoire de l'enrichissement de l'uranium, 1973–1993* ([Anvers]: Fonds Mercator, 1993): 169.
8. International Panel on Fissile Materials, *Balancing the Books: Production and Stocks*, *op. cit.*, 86.
9. Jean-Pierre Daviet, *Eurodif: Histoire de l'enrichissement de l'uranium, 1973–1993*, *op. cit.*, 169.
10. International Panel on Fissile Materials, *Balancing the Books: Production and Stocks*, *op. cit.*, 85.
11. Claude Frejacques et al., “Principal Results Obtained in France in Studies of the Separation of the Uranium Isotopes by Gaseous Diffusion,” 4 (presented at the second United Nations international conference on the peaceful uses of atomic energy, Geneva, 1959): 418–421.
12. KREBS, Etablissement de Pierrelatte. Butte de Stockage: Reconnaissance et Etude d'Impact, (May 1998) 4, <www.aveva.com/activities/liblocal/docs/BG%20amont/monde/tricastin/Rapport_Krebs_butte%20de%20stockage.pdf>.
13. Cogema, “Pierrelatte A Bien Redémarré,” *Cogemagazine* 24 (1985): 5.
14. Didier Chauvet, Ordonnancement de la maintenance des usines de diffusion gazeuse et de la distribution électrique (Etablissement de Pierrelatte: Cogema, 19 April 1990), 1.
15. Pascal Bourrelier and Charles Kassel, *op. cit.*, 40.
16. Daniel Massignon, “Gaseous Diffusion,” in *Uranium Enrichment*, ed. Stelio Villani, 35 (Berlin, Heidelberg: Springer Berlin Heidelberg, 1979), 55–182.
17. Pascal Bourrelier and Charles Kassel, *op. cit.*, 37.
18. Jean-Pierre Daviet, “Eurodif: Histoire de l'enrichissement de l'uranium, 1973–1993,” *op. cit.*, 193.
19. Pierre Plurien and Jean-Hubert Coates, “La diffusion gazeuse en France de Pierrelatte à Eurodif,” *Revue Générale Nucléaire* 2 (March 1996): 11–16.
20. Paul Dreyfus, “Pierrelatte, l'usine-mystère ouvre ses portes à la presse,” *Le Dauphiné Libéré*, 28 March 1964.
21. Paul Dreyfus, “M. Gaston Palewski a inauguré l'usine basse de Pierrelatte,” *Le Dauphiné Libéré*, January 21, 1965.
22. Jean-Pierre Daviet, *Eurodif: Histoire de l'enrichissement de l'uranium, 1973–1993*, *op. cit.*, 196.
23. C. Leduc et al., “Acquis Français en Matière de Séparation Isotopique,” Vol. 9, presented at the fourth United Nations international conference on the peaceful uses of atomic energy, New York (1972), 15–29.
24. Jean-Pierre Daviet, *Eurodif: Histoire de l'enrichissement de l'uranium, 1973–1993*, *op. cit.*, 194.
25. Claude Frejacques et al. , *op. cit.*, 421.
26. Jean-Pierre Daviet, *Eurodif: Histoire de l'enrichissement de l'uranium, 1973–1993*, *op. cit.*, 195.
27. “Cogéma: Le secret dévoilé,” *La Tribune*, 2 November 1995, 11.
28. *Ibid.*

29. International Panel on Fissile Materials, *Balancing the Books: Production and Stocks*, *op. cit.*, 87; David Albright, Frans Berkhout, and William Walker, *Plutonium and Highly Enriched Uranium, 1996: World Inventories, Capabilities, and Policies* (SIPRI, 1997): 122–126.
30. KREBS, *Etablissement de Pierrelatte. Butte de Stockage: Reconnaissance et Etude d'Impact*, *op. cit.*, 4.
31. Jean Claude Guais, “Hierarchical Optimization in Isotope Separation—Gaseous Diffusion Plant-cascade-stage—Principle and Applications,” in *Proceedings of the International Conference Organised by the British Nuclear Energy Society in Conjunction with Kerntechnische Gesellschaft* (presented at the Uranium isotope separation, London: The British Nuclear Energy Society, 1976): 151–164.
32. For the equations used to calculate the ideal cascade see Bruno Brigoli, “Cascade Theory,” in *Uranium Enrichment*, ed. Stelio Villani, vol. 35 (Berlin, Heidelberg: Springer Berlin Heidelberg, 1979): 24–28.
33. Equations used to produce the squared-off cascade are derived from the theory presented in Karl Cohen, *The Theory of Isotope Separation as Applied to the Large-Scale Production of U-235* (New York: McGraw-Hill, 1951): 1–165 and Bruno Brigoli, *op. cit.*, 47–51. In this model, the criterion used to optimize the cascade shape consists to minimize the total flow rate of every step per mole of product.
34. International Panel on Fissile Materials, *Balancing the Books: Production and Stocks*, *op. cit.*, 87.
35. Pierre Plurien and Jean-Hubert Coates, *op. cit.*, 11.
36. Randall D. Scheele et al., “Development of NF₃ Deposit Removal Technology for the Portsmouth Gaseous Diffusion Plant,” in *WMS Papers (presented at the Waste Management Symposia, Tucson, AZ, 2006)*: 1–15, <www.wmsym.org/archives/2006/pdfs/6297.pdf>.
37. Daniel Massignon, *op. cit.*, 125.
38. G. Menard et al., “Filtration Tangentielle des Gaz: Etude de la Formation du Dépôt,” *Powder Technology* 71, (September 1992): 263–272.
39. Pascal Bourrelier and Charles Kassel, *op. cit.*, 41.
40. Fluor-B&W Portsmouth LLC, “Expression of Interest: Recycling of Portsmouth GDP Radiologically Contaminated Nickel,” 2012, 1–6, <www.fbportsmouth.com/17docs/Solicitations/3-23-12%20Final%20FBP%20Ni%20EOI.pdf>.
41. At that point, particles re-entrainment due to an increasing shear velocity at the gas/deposit interface balances the amount of newly trapped particles stopping further growth of the deposit layer.
42. G. Menard et al. , *op. cit.*
43. The impact of the water-regeneration cycle on the particle concentration is difficult to assess and remains unknown to the authors.
44. The air temperature and pressure inside the process building are assumed to be 55°C and 1 atmosphere. No data on the air relative humidity were found. A value of 15% will be taken for the calculations assuming a relatively dry and monitored atmosphere in the process building.
45. Claude Frejacques et al. , *op. cit.*, 420; Daniel Massignon, *op. cit.*, 137.
46. Commissariat à l’Energie Atomique, *CEA Rapport Annuel, (1967)*: 1–217.
47. KREBS, *Etablissement de Pierrelatte. Butte de Stockage: Reconnaissance et*

Etude d'Impact, *op. cit.*, 4.

48. Ibid.

49. Ibid.

50. Jean-Pierre Daviet, *Eurodif: Histoire de l'enrichissement de l'uranium, 1973–1993*, *op. cit.*, 207.

51. KREBS, Etablissement de Pierrelatte. Butte de Stockage: Reconnaissance et Etude d'Impact, *op. cit.*, 4.

52. This amount would be equivalent to 1.6×10^{10} one-micrometer diameter spherical particles trapped per year in every tubular membrane.

53. This rate is about three hundred times smaller than the rate calculated from the buried first generation barriers. This indicates clearly that the process in the Pierrelatte plant was not working as designed or specified during the first years of operation. This eventually led to the replacement of all the tubular membranes (over 5 millions) in UB only 2.5 years after the production had started.

54. Alexander Glaser and Stefan Bürger, "Verification of a Fissile Material Cutoff Treaty: The Case of Enrichment Facilities and the Role of Ultra-trace Level Isotope Ratio Analysis," *Journal of Radioanalytical and Nuclear Chemistry* 280, 1 (April 1, 2009): 85–90.

55. Committee on Decontamination and Decommissioning of Uranium Enrichment Facilities, National Research Council, *Affordable Cleanup?*, *op. cit.*, 52.

56. Pascal Bourrelier and Charles Kassel, *op. cit.*, 41.

57. Fanny Jallu et al., "Dismantling and Decommissioning: The Interest of Passive Neutron Measurement to Control and Characterise Radioactive Wastes Containing Uranium," *Nuclear Instruments and Methods in Physics Research Section B: Beam Interactions with Materials and Atoms* 271 (January 15, 2012): 48–54.

58. Committee on Decontamination and Decommissioning of Uranium Enrichment Facilities, National Research Council, *Affordable Cleanup?*, *op. cit.*, 51.

59. S.G. Baxter and P. Bradbury, *op. cit.*

60. See the website <www.dechets-radioactifs.com/les-dechets-radioactifs/classification/dechets-tfa.html>, edited by the French Agency for the Radioactive Wastes Management (ANDRA).

61. COGEMA, Dossier de demande d'autorisation des rejets d'effluents liquides et gazeux radioactifs et non radioactifs, Titre 2, (INBS-COGEMA-PIERRELATTE, 2000): 31.

62. Daniel Massignon, *op. cit.*, 55.

63. Daniel Massignon, *op. cit.*, 57.

64. Jean-Pierre Daviet, *Eurodif: Histoire de l'enrichissement de l'uranium, 1973–1993*, *op. cit.*, 21.

65. Karl Cohen, The Theory of Isotope Separation as Applied to the Large-Scale Production of U-235, *op. cit.*, 29.

APPENDIX A: INTRODUCTION TO THE GASEOUS DIFFUSION PROCESS

Gaseous diffusion is an isotope separation method based on the molecular diffusion of a gaseous isotopic mixture through porous barriers (or membranes). In the case of uranium isotope separation, the processed gas is a mixture of uranium-238 and uranium-235 in uranium hexafluoride, UF_6 .

In a closed cell in thermal equilibrium condition, all molecules of an isotopic mixture have the same kinetic energy. On average, for the same temperature, lighter molecules will travel faster and thus hit the surrounding walls more often. If one of the boundary conditions is represented by a porous barrier that has small enough pores to avoid the outflow of the gas but can still allow molecular diffusion, the fraction of the gas that will go through the barrier will be enriched with a higher ratio of the lighter isotopes.⁶²

Figure 7 shows an elementary diffusion stage, the dashed line represents the diffusion barrier. The couples (N, L) , $(N', L' = \theta L)$ and $(N'', L'' = (1 - \theta)L)$ are respectively the composition and molar flow rate of the feed flow, the enriched flow, and the depleted flow with θ being the “cut” of the cell. The typical value of the cut is 0.5 meaning that half of the processed gas is slightly enriched in the lighter isotopes at the cell output.

The ideal separation factor, which defines the concentration change in the gas mixture of uranium hexafluoride across a stage, is given by the ratio of the Maxwell mean velocities of the two isotopes in the hexafluoride form:⁶³

$$\alpha_0 = \frac{N'}{(1 - N')} \frac{(1 - N)}{N} = \frac{\bar{v}_1}{\bar{v}_2} = \sqrt{\frac{M_2}{M_1}} = \sqrt{\frac{352}{349}} = 1.00429 \quad (\text{A.1})$$

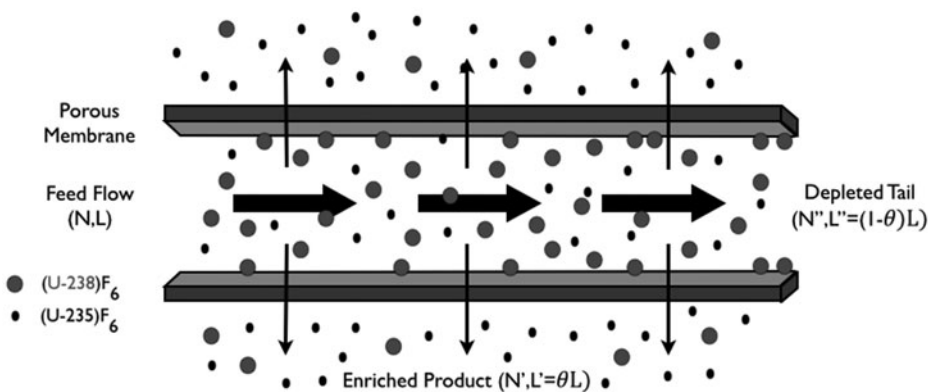


Figure 7: Elementary diffusion stage.

In reality, the separation factor α of a single stage will be lower than the ideal separation factor α_0 due to the efficiency factor of the barrier. Usual barriers will not have a separation factor higher than $\alpha = 1.0022$.⁶⁴

This separation factor being so small, in order to enrich the gas composition in uranium-235 to a level required for use in nuclear weapons (over 90% uranium-235), the uranium hexafluoride needs to be processed through a multitude of inter-connected stages or a cascade (typically of the order of a few thousands stages).

APPENDIX B: SOLUTION OF THE STAGE EQUATION FOR A SQUARED-OFF CASCADE

Fundamental Equation of Isotope Separation

The fundamental equation of isotope separation describes the approach towards equilibrium of a cascade:⁶⁵

$$H \frac{\partial N}{\partial t} = \frac{\partial}{\partial s} \left[\frac{L}{2} \frac{\partial N}{\partial s} - (\alpha - 1)LN(1 - N) - PN \right] \quad (\text{B.1})$$

with H being the total hold-up of the plant, N the isotopic concentration which is a function of time t and stage s , α the separation factor, L the material flow as a function of stage and P the product flow of the plant.

For the case of a squared-off cascade, the material flow L is constant and independent of the stage number for every step, and assuming steady-state operation, the quasi-linear parabolic equation (B.1) becomes:

$$\frac{L}{2} \frac{\partial^2 N}{\partial s^2} - (\alpha - 1)L \frac{\partial}{\partial s} (N(1 - N)) - P \frac{\partial N}{\partial s} = 0 \quad (\text{B.2})$$

Integrating equation (B.2) once with respect to s , gives:

$$-\frac{L}{2} \frac{\partial N}{\partial s} + (\alpha - 1)LN(1 - N) + PN = PN_P \quad (\text{B.3})$$

with N_P the isotopic concentration of the product flow. Finally, integrating a second time:

$$\int ds = \frac{L}{2} \int \frac{dN}{(\alpha - 1)LN(1 - N) + PN - PN_P} \quad (\text{B.4})$$

gives the following solution to equation (B.2):

$$s = \frac{1}{(\alpha - 1)\Delta(\psi)} \tanh^{-1} \left[\frac{(N_s - N_0)\Delta(\psi)}{(N_s + N_0)(1 + \psi) - 2N_s N_0 - 2\psi N_P} \right] \quad (\text{B.5})$$

With N_O the concentration of the feed flow and ψ the normalized production rate (dimensionless number) given by

$$\psi = \frac{P}{(\alpha - 1)L} \quad (\text{B.6})$$

$\Delta(\psi)$ being the following defined operator:

$$\Delta(\psi) = [1 + \psi^2 + 2\psi N_P]^{1/2} \quad (\text{B.7})$$

Single Step Square Symmetric Cascade Equation

For a single step square symmetric cascade, with $s = S$ the total number of stage and $N_s = N_P$, the stage equation is given by the following transcendental equation:

$$S = \frac{1}{(\alpha - 1)\Delta(\psi)} \tanh^{-1} \left[\frac{(N_P - N_0)\Delta(\psi)}{(N_P + N_0)(1 + \psi) - 2N_P N_0 - 2\psi N_P} \right] \quad (\text{B.8})$$

There is an infinite number of couple (S, ψ) that satisfied equation (B.8), which corresponds to the variation of ψ from zero to ψ_{max} with

$$\psi_{max} = \frac{N_0(1 - N_0)}{N_P - N_0} \quad (\text{B.9})$$

Optimization of a Squared-off Cascade with Multiple Steps

For the enrichment section, considering the i th step of the cascade, the equation (B.5) becomes

$$S_i = \frac{1}{(\alpha - 1)\Delta(\psi_i)} \tanh^{-1} \left[\frac{(N_i - N_{i-1})\Delta(\psi_i)}{(N_i + N_{i-1})(1 + \psi_i) - 2N_i N_{i-1} - 2\psi_i N_P} \right] \quad (\text{B.10})$$

with N_i and N_{i-1} being the product and feed concentration of the i -th step.

The criterion used to optimize equation (B.10) in this paper consist to minimize the total flow rate per mole of product,

$$\text{Criterion} = \min \left(\frac{LS}{P} \right) \quad (\text{B.11})$$

with

$$\frac{LS}{P} \propto \frac{S}{\psi} \quad (\text{B.12})$$

Thus the optimum conditions of the i -th step are given by

$$\frac{d}{d\psi_i} \left(\frac{S_i}{\psi_i} \right) = 0 \quad (\text{B.13})$$

Using the expression of S_i in equation (B.10), equation (B.13) becomes

$$\begin{aligned} & \left[\Delta(\psi_i) + \frac{\psi_i(1 + \psi_i - N_P)}{\Delta(\psi_i)} \right] \tanh^{-1} \left(\frac{U}{V} \right) \\ &= \frac{1}{V^2 - U^2} \psi_i [(N_i - N_{i-1})(1 + \psi_i - 2N_P)V - \Delta(\psi_i)(N_i + N_{i-1} - 2N_P)U] \end{aligned} \quad (\text{B.14})$$

with

$$U = (N_i - N_{i-1}) \Delta(\psi_i) \quad (\text{B.15})$$

and

$$V = (N_i + N_{i-1})(1 + \psi_i) - 2N_i N_{i-1} - 2\psi_i N_P \quad (\text{B.16})$$

The optimum value of ψ_i is obtained from the equation (B.14), and then used to solve equation (B10) to obtain the optimum S_i .

Stage Equation in the Stripping Section

The couples (S_i, ψ_i) in the stripping section are obtained with the same set of equations, by replacing respectively P and N_P by $-W$, the tail flow rate, and N_W , the tail concentration:

$$S_i = \frac{1}{(\alpha - 1)\Delta(\psi_i)} \tanh^{-1} \left[\frac{(N_i - N_{i-1})\Delta(\psi_i)}{(N_i + N_{i-1})(1 + \psi_i) - 2N_i N_{i-1} - 2\psi_i N_W} \right] \quad (\text{B.17})$$

and,

$$\psi_i = \frac{-W}{(\alpha - 1)L} \quad (\text{B.18})$$

APPENDIX C: UO_2F_2 PARTICLES CONCENTRATION IN UF_6 FLOW

Particles of UO_2F_2 are obtained from the hydrolysis of UF_6 by water following the reaction:



The source of water entering the process is the in-leakage of air surrounding the equipment. The rate flow of air, \dot{a} , entering a vessel by porosity is expressed in liters per second at the pressure of one millitor or *lusec*. Plant designers will usually fix a very low value of admissible leak rate for all the equipment in *lusec* per m^3 of UF_6 .

A *lusec* is the product of a pressure and a volume divided by time. If air is assumed to behave as a perfect gas, then the molar flow of air entering the equipment, \dot{n}_{air} , is given by

$$\dot{n}_{air} = \frac{\dot{a}}{RT} \quad (\text{C.2})$$

with R the perfect gas constant and T the average temperature in the process building.

The total pressure of a perfect gas mixture is the sum of the partial pressures of all the components:

$$P_{air} = P_{H_2O} + P_{dryair} \quad (C.3)$$

With

$$\frac{P_{H_2O}}{P_{air}} = \frac{n_{H_2O}}{n_{air}} \quad (C.4)$$

The partial pressure of water, P_{H_2O} , in air is obtained by multiplying the relative humidity ϕ of the air inside the building by P_{vap} the water vapor pressure at the average temperature, T of the process building using the Clapeyron formula,

$$\ln\left(\frac{P_{vap}}{P_0}\right) = \frac{ML_v}{R} \left(\frac{1}{T_0} - \frac{1}{T}\right) \quad (C.5)$$

with M the molar mass of water, L_v the latent heat of vaporization, P_0 and T_0 respectively pressure and temperature of the boiling point.

The molar flow of water entering the equipment, \dot{n}_{H_2O} , is then given by,

$$\dot{n}_{H_2O} = \dot{n}_{air} \frac{\phi P_{vap}}{P_{air}} \quad (C.6)$$

Assuming that all moles of water will react with UF_6 , the average UO_2F_2 particle concentration in the flow is given by

$$C = \frac{1}{2} \frac{\dot{n}_{H_2O} M_{UO_2F_2}}{Q_{UF_6}} \quad (C.7)$$

with $M_{UO_2F_2}$ the molar mass of UO_2F_2 and Q_{UF_6} the volumetric flow rate of UF_6 .